

CARTOGRAPHY OF THE ICY SATURNIAN SATELLITES

T. Roatsch¹, J. Oberst¹, B. Giese¹, M. Wählisch¹, V. Winkler¹, K.-D. Matz¹, R. Jaumann¹, G. Neukum²

- 1) Institute of Planetary Research, German Aerospace Center; Rutherfordstr. 2; D-12489 Berlin; Germany (please direct all correspondence to: T. Roatsch, thomas.roatsch@dlr.de)
2) Freie Universität, Institute for Geosciences, Berlin, Germany

ABSTRACT

We have re-measured control points and re-computed a control point network for Saturn's satellite Dione. Our network is based on 16 images (obtained by the narrow-angle cameras of Voyager I and II), 135 control points, and 741 point measurements. We obtained mean point accuracies of 1.8 km, 2.9 km, and 1.2 km for X, Y, and Z, respectively. The radius of Dione was re-determined to be 562.5 km \pm 0.2 km with a RMS deviation of 3 km, consistent with 560 km (RMS: 5 km) found by Davies et al. 1983. Subsequently, we generated a sequence of controlled digital base mosaics for the five (among the largest) satellites Mimas, Enceladus, Tethys, Dione, and Rhea. The images are reprojected in Mercator and Polar Stereographic projections using satellite shape parameters, as recommended by IAU. On the basis of these mosaics, maps in printable format have been produced. Our data products update previous control point networks and maps of these satellites, released by the RAND Corporation and the USGS (United States Geological Survey), respectively, between 1982 and 1992. Our maps constitute an important basis for the planning of the Cassini mission, which will begin its orbital tour through the Saturnian system in June 2004 (<http://saturn.jpl.nasa.gov>).

1. INTRODUCTION

The Cassini spacecraft is preparing to enter orbit about Saturn on July, 1st, later this year, and will then carry out a comprehensive exploration and mapping program of its icy satellites. Motivated by these future prospects, we are presently carrying out a comprehensive photogrammetric and cartographic study of these satellites, using images obtained by the Voyager-1 and -2 spacecraft during their Saturn flybys in 1980 and 1981

(<http://www.jpl.nasa.gov/voyager>). The satellites are locked in synchronous rotation and exposed to strong tidal and rotational forces; therefore, they have assumed a strong ellipsoidal shape. In addition, owing to the restricted viewing geometry during the two fast flybys, the effective image resolution varies strongly over the surface of each satellite. Thus, any cartography work on these satellites is far from routine and requires non-standard methods of image processing.

	Mean radius	Equatorial radius (subplanetary)	Equatorial radius (along-orbit)	Polar radius
	km	km	km	km
Mimas	198.6 \pm 0.6	209.1 \pm 0.5	196.2 \pm 0.5	191.4 \pm 0.5
Enceladus	249.4 \pm 0.3	256.3 \pm 0.3	247.3 \pm 0.3	244.6 \pm 0.5
Tethys	529.8 \pm 1.5	535.6 \pm 1.2	528.2 \pm 1.2	525.8 \pm 1.2
Dione	560 \pm 5 *)	--- **)		
Rhea	764 \pm 4	--- **)		

*) revised in this study: $r = 562.5 \pm 0.2$ km

***) no tri-axial shape parameters available

Table 1: IAU shape parameters (Seidelmann et al., 2003)

From the large number of available Voyager images, we selected a small number with appropriate coverage and image quality (see Appendix, Table A1). Though Voyager had obtained many narrow band filter images, only clear filter images were used in our processing. All Voyager images are available online from the Planetary Data System (PDS) Imaging Node (<http://pds-imaging.jpl.nasa.gov>). The images were initially converted from PDS to VICAR (Video Image Communication And Retrieval, <http://rushmore.jpl.nasa.gov/vicar.html>) format and radiometrically calibrated to account for dark current and flat field. The images were then geometrically calibrated using reseau mark measurements and standard resampling methods (Benesh and Jepsen, 1978; see <http://www-mipl.jpl.nasa.gov/external/vicar.html>

for details) to compensate for the intrinsic geometric distortion of the Vidicon sensor.

2. DIONE

Control point networks and maps of the satellites of Saturn have been released earlier by the RAND Corporation Davies and Katayama (1983a,b,c; 1984) and the USGS (United States Geological Survey). We first focused on the satellite Dione, for which (except perhaps Rhea) the best image data are available.

2.1 Control point network

The earlier control point work for Dione (Davies and Katayama, 1983) involved image point measurements in 27 Voyager-1 images (1-16 km per pixel) and one Voyager-2 image (5 km per pixel) to determine the latitudes and longitudes of 126 ground control points. Along with the 2D-coordinates of the control points Davies and Katayama determined the radius of Dione and defined the position of the prime meridian.

We re-computed this control point network using a subset of 15 Voyager-1 images with resolutions better than 9 km/pixel and the one Voyager-2 image. Within our calculations, the position of the prime meridian was fixed at the value determined by Davies and Katayama (1983). However, rather than determining the latitudes and longitudes of the control points only, we solved for the full 3D-coordinates (X, Y, Z) of each control point (Zeitler and Oberst, 1999; Oberst and Schuster, 2004). This approach potentially allowed us to determine a higher-order figure of Dione beyond the sphere.

Over all, there were 135 points (Fig. 1) that were measured in the 16 images. The total number of image point measurements was 1482. Image coordinates were converted to mm on the focal plane using established camera calibration data (Table 2). Due to the fact that the surface areas of Dione were mapped at different image resolutions (see the varying detail across the map) the ability to identify points was strongly affected. As a result, the distribution of the points is far from uniform, with a broad point gap to the west and poor coverage towards the poles.

Using bundle block adjustments, we determined the surface coordinates of the control points. Image point measurements and the camera pointing data were introduced as observations with standard deviations of 9 micro m and 1 mrad, respectively. The camera positions were taken fixed at their nominal values. In addition, Dione's center of figure was introduced as a ground control point with X=Y=Z=0. This center of figure was determined from the position of the limb, which was measured by a limb-fitting program.

The limb was clearly visible in most Dione images. The X-, Y-, and Z-coordinates of the control points and the three pointing angles of each image were treated as unknowns and were solved for.

As a result of the block adjustment we obtained mean point accuracies of 1.8 km, 2.9 km, and 1.2 km for X, Y, and Z, respectively. The lowest point accuracies are 3.5 km, 6.8 km, and 2.5 km (X, Y, and Z) and belong to those points located only within the 5-9 km resolution images (Fig. 2).

K, pix/mm	84.8214	
s ₀ , pix	500.5	
l ₀ , pix	500.5	
f, mm	VGR1-NAC	1500.19
	VGR1-WAC	200.465
	VGR2-NAC	1503.49
	VGR2-WAC	200.770

Camera parameters are taken from standard navigation data files (<http://naif.jpl.nasa.gov/naif.html>) and refer to the geometrically corrected images

Table 2: Voyager Camera Parameters

2.2 Global Shape

The 3D-coordinates of the control points allowed us to determine the global shape of Dione. The poor point coverage of the body (Fig. 1) suggests considering only very simple body models. Following methods described by Oberst and Schuster (2004), we performed least-squares fits to the data using a sphere, a 2-axial ellipsoid, and a 3-axial ellipsoid, taking into account the radial point errors as weights in the fitting (Fig. 3). In result we obtained a RMS value of about 3 km in each case suggesting that a sphere described the shape of the body sufficient well, and that it was not meaningful to proceed to higher-order models. Within this model the radius of Dione was determined to be R=562.5 +/- 0.2 km consistent with R=560 (RMS=5 km) determined by Davies and Katayama (1983).

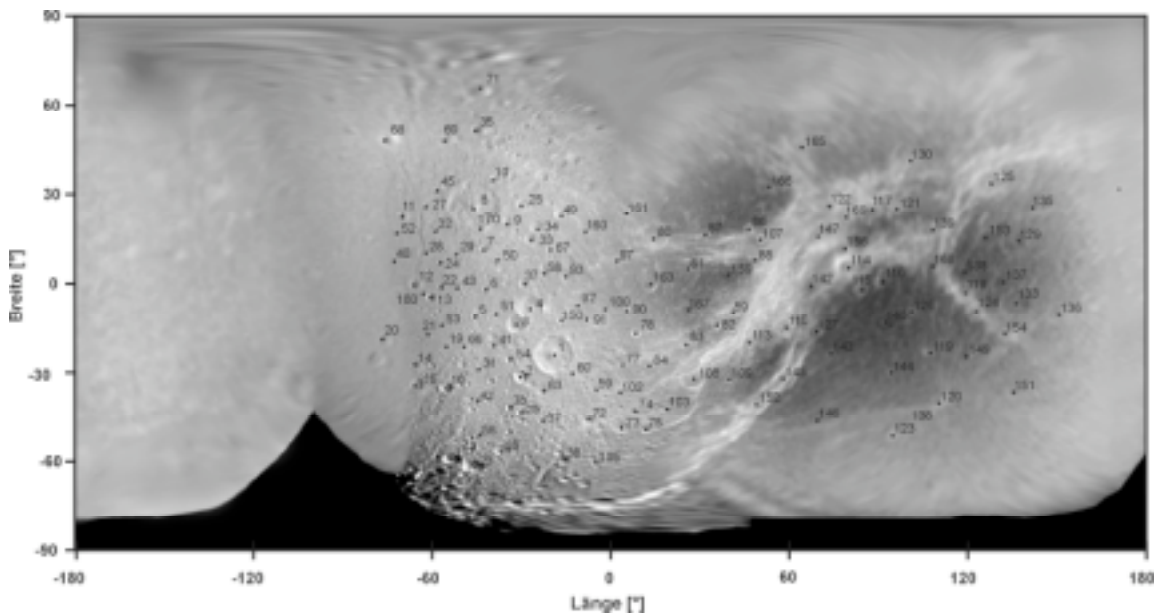


Fig. 1: Dione base map showing the distribution of the control points.

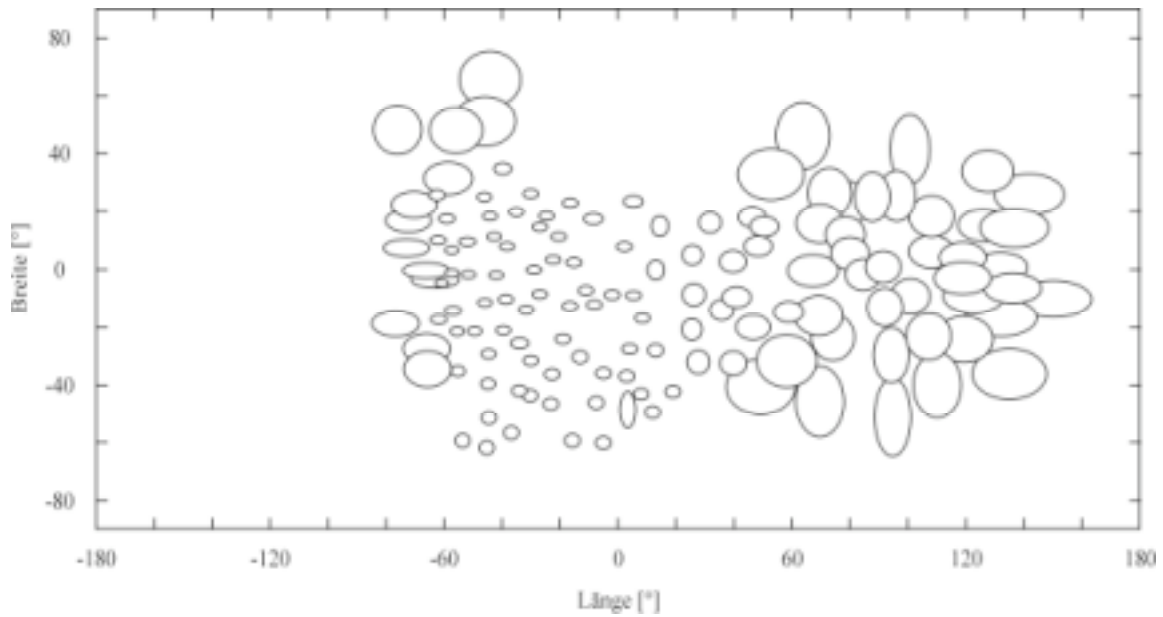


Fig. 2: Horizontal error ellipses of the control points, with the lengths of the ellipse axes proportional to the errors. The largest ellipse has a size of 13.6 km. Compare the sizes of the error ellipses with the image resolutions (Fig. 1)!

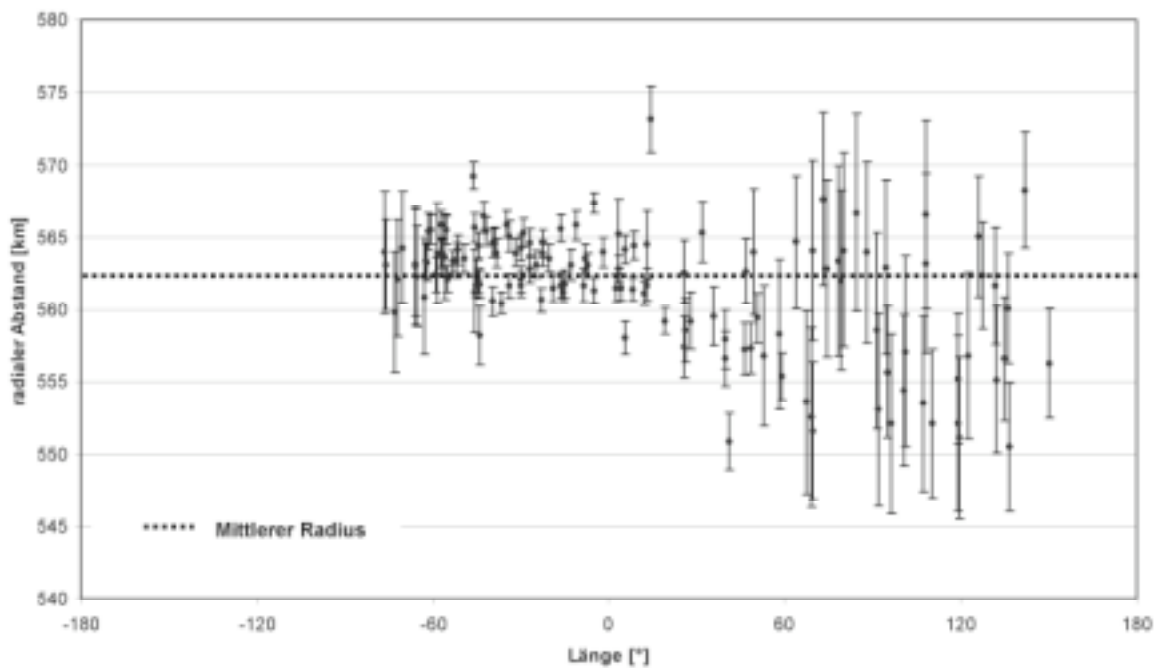


Fig. 3: Radial distances and errors for the control points of Dione

3. DIGITAL IMAGE MOSAICS

Image mosaics and maps were produced for the five largest satellites (excluding the cloud-shrouded satellite Titan) Mimas, Enceladus, Tethys, Dione, and Rhea. The images were first reprojected to digital maps, using orbit and pointing data derived by Davies and Katayama (1983a,b,c; 1984). However, for Dione images, improved pointing data were taken from limb-fitting procedures mentioned above.

For comparison and interpretation of the maps, a 3-axial ellipsoid was used for the calculation of the ray intersection point; however, the map projections were done on a sphere, with all satellite shape parameters taken from IAU recommendations (Seidelmann et al., 2003, see Table 1). A photometric correction using the Minnaert function was applied to every image during map projection.

The final step of the image processing was the combination of all map-projected images (14, 9, 8, 13, and 37 Voyager-1 images, for Mimas, Enceladus, Tethys, Dione, and Rhea, respectively) to a homogeneous mosaic. Special care had to be taken to the different ground resolution of the input

images within the overlapping regions so to minimize the loss of high resolution image information. In addition, illumination conditions varied from image to image, and image brightness had to be adjusted to avoid visible seams.

Both, map projection and mosaicking software, originally developed at DLR (Scholten, 1996), are currently improved for the upcoming data processing of the Cassini-ISS images. These digital image mosaics will be released in PDS format.

4. MAPS

The printed maps for the above-named satellites were produced taking the controlled photomosaics as a basis. They conform with the layout of the USGS maps (Map I-1921, I-2155, I-2156, I-2157, I-2158) to facilitate comparisons. Map projections are conformal: Within the latitude range from -57° to 57° , the Mercator projection was used. The poles are projected in polar stereographic projection. The prime meridian on the Saturn-facing hemisphere is in the center of the map. The grid system is showing planetocentric latitudes and West longitudes.

	Equatorial Regions*)	Poles
Mimas	1:200,000	1:1,000,000
Enceladus	1:200,000	1:1,000,000
Tethys	1:500,000	1:3,000,000
Dione	1:500,000	1:3,000,000
Rhea	1:500,000	1:3,000,000

*) $-57^\circ < \text{Latitude} < +57^\circ$

Table 3: Map scales

Names of geological features (e.g., crater, lineae, chasmae, fossae) were added in the maps and follow the official IAU-nomenclature (Greeley, R., Batson, R.M., 1990, USGS 2004). Printable versions of the maps in PDF-format will be released.

5. OUTLOOK FOR CASSINI

The Cassini spacecraft will go on a four-year tour through the Saturnian system, beginning with the close flyby of the outer satellite Phoebe in June of this year. Observations will be carried out by the Cassini's onboard ISS (Imaging Subsystem), which consists of a high-resolution and a wide-angle camera. Highest resolution images will be taken during the close flybys (between 500 and 2000 km), planned for all icy satellites except Mimas, and during other non-targeted flybys (distance $< 50,000$ km). We plan to improve both the image maps and the control point networks on a regular basis. Fig. 4 shows the planned coverage of Dione during the first three years of the tour, as an example.

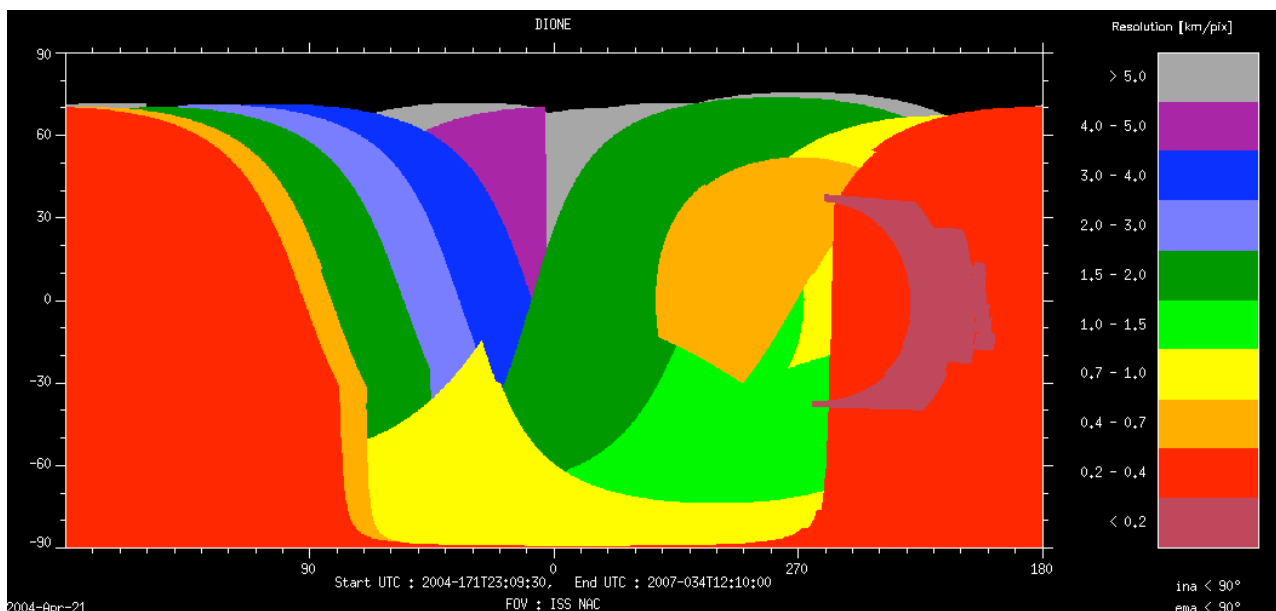


Fig. 4: Coverage of Dione that will be accomplished by Cassini between 2004 and 2007

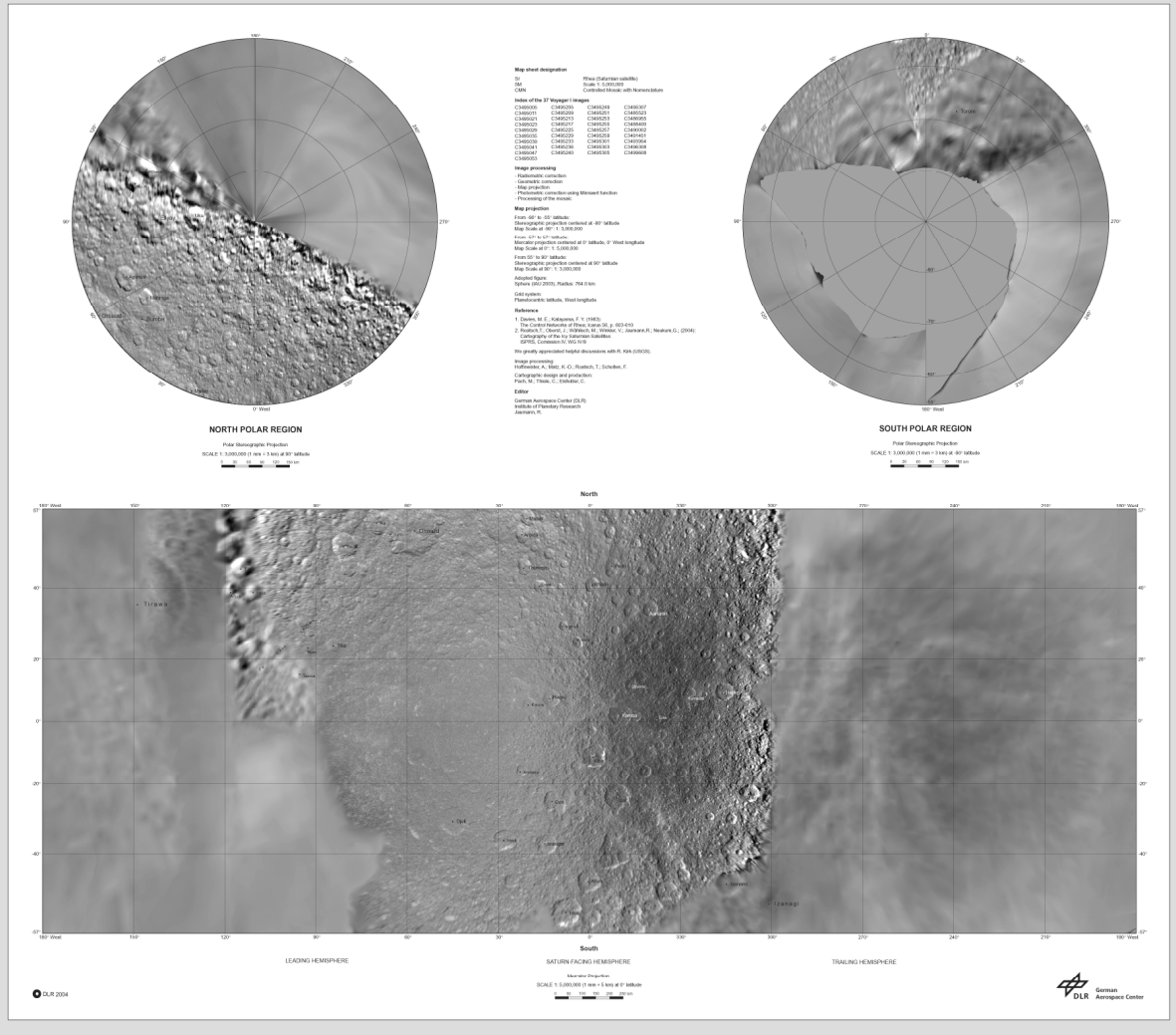


Fig. 5: Controlled photomosaic of Rhea. Similar maps are available for Dione, Enceladus, Mimas, and Tethy

REFERENCES

Benesh, M. and P. Jepsen, 1978, Voyager Imaging Science Subsystem Calibration Report, California Institute of Technology, Jet Propulsion Laboratory Publication 618-802, July 31.

Davies, M. E. and Katayama, F. Y., 1983a, The control networks of Tethys and Dione, *J. Geophys. Res.* 88, pp. 8729-8735.

Davies, M. E. and Katayama, F. Y., 1983b, The control networks of Mimas and Enceladus, *Icarus* 53, pp. 332-340.

Davies, M. E. and Katayama, F. Y., 1983c, The control network of Rhea, *Icarus* 56, pp. 603-610.

Greeley, R., Batson, R.M., 1990. *Planetary Mapping*. Cambridge University Press.

Oberst, J. and P. Schuster, 2004, The vertical control point network and global shape of Io, *J. Geophys. Res.*, in press.

Scholten, F., 1996, Automated Generation of Coloured Orthoimages and Image Mosaics Using HRSC and WAOSS Image Data of the Mars96 Mission, International Archives of Photogrammetry and Remote Sensing, Vol. XXXI, Part B2, S.351-356, Wien

Seidelmann et al., Report of the IAU/IAG working group on cartographic coordinates and rotational elements of the

planets and satellites: 2000, *Celestial Mechanics and Dynamical Astronomy*, Vol. 82, Issue 1, 83-111, 2002.

Zeitler, W. and J. Oberst, 1999, The Mars Pathfinder Landing Site and the Viking Control Point Network, *J. Geophys. Res.* 104 (E4), pp. 8935-8941.

Map I-1921 Saturn, Rhea, Digital Map, Photomosaics,
Map I-2155 Saturnian Satellites, Pictorial Map of Mimas
Map I-2156 Saturnian Satellites, Pictorial Map and
Controlled Photomosaics of Enceladus
Map I-2157 Saturnian Satellites, Pictorial Map and
Controlled Photomosaics of Tethys
Map I-2158 Saturnian Satellites, Pictorial Map and
Controlled Photomosaics of Enceladus

ACKNOWLEDGEMENTS

The authors acknowledge helpful discussions with R. Kirk (USGS). Printable versions of the maps are available from the authors on request.

APPENDIX A/ IMAGE LIST

Mimas: (Voyager-1 and -2)

C3493040 C3493204 C3493350
C3493615 C3493818 C3494034
C3494421 C4396651 C4398225
C4398902 C4400404

Enceladus: (Voyager-1 and -2)
C3493343 C4398906 C4399312
C4398323 C4400432 C4400436
C4399737 C3492956 C4400042

Tethys: (Voyager-1 and -2)
C3490252 C3490730 C3492618
C3493706 C4396809 C4397511
C4398021 C4398857 C4399558
C4400357 C4400732

Dione: (Voyager-1 and -2)
C3490043 C3490807 C3491411
C3492526 C3493338 C3494458
C3494816 C3494822 C3494828
C4394304 C4396336 C4397721
C4399616

Rhea: (Voyager-1 only)
C3495005 C3495011 C3495021
C3495023 C3495029 C3495035
C3495039 C3495041 C3495047
C3495053 C3495205 C3495209
C3495213 C3495217 C3495225
C3495229 C3495233 C3495236
C3495240 C3495249 C3495251
C3495253 C3495255 C3495257
C3495259 C3495301 C3495303
C3495305 C3495307 C3485523
C3486955 C3488400 C3490002
C3491451 C3493954 C3496308
C3499608

Table A1: List of Voyager Images